Mechanisms of Development 159 (2019) 103568

Contents lists available at ScienceDirect

Mechanisms of Development

journal homepage: www.elsevier.com/locate/mod

An in vitro model of region-specific rib formation in chick axial skeleton: Intercellular interaction between somite and lateral plate cells

Kaoru Matsutani[a], Koji Ikegami[a], Hirohiko Aoyama[a,b,*]

[a] Department of Anatomy and Developmental Biology, Graduate School of Biomedical and Health Sciences, Hiroshima University, 1-2-3 Kasumi, Minami-ku, Hiroshima 734-8553, Japan

[b] Department of Medical Science and Technology, Faculty of Health Sciences, Hiroshima International University, 555-36 Kurosegakuendai, Higashihiroshima City, Hiroshima 739-2695, Japan

ARTICLE INFO

Keywords:
Chick
Somite
Lateral plate
Intercellular interaction
Axial skeleton
Morphogenesis

ABSTRACT

The axial skeleton is divided into different regions based on its morphological features. In particular, in birds and mammals, ribs are present only in the thoracic region. The axial skeleton is derived from a series of somites. In the thoracic region of the axial skeleton, descendants of somites coherently penetrate into the somatic mesoderm to form ribs. In regions other than the thoracic, descendants of somites do not penetrate the somatic lateral plate mesoderm. We performed live-cell time-lapse imaging to investigate the difference in the migration of a somite cell after contact with the somatic lateral plate mesoderm obtained from different regions of anterior–posterior axis in vitro on cytophilic narrow paths. We found that a thoracic somite cell continues to migrate after contact with the thoracic somatic lateral plate mesoderm, whereas it ceases migration after contact with the lumbar somatic lateral plate mesoderm. This suggests that cell–cell interaction works as an important guidance cue that regulates migration of somite cells. We surmise that the thoracic somatic lateral plate mesoderm exhibits region-specific competence to allow penetration of somite cells, whereas the lumbosacral somatic lateral plate mesoderm repels somite cells by contact inhibition of locomotion. The differences in the behavior of the somatic lateral plate mesoderm toward somite cells may confirm the distinction between different regions of the axial skeleton.

1. Introduction

Cell migration is considered one of the fundamental processes in embryo morphogenesis (Le Douarin, 1984; Reig et al., 2014). Cell migration behavior can change by some signals, and depending on the source of the signal and the way it is received. Signaling mechanisms are classified into chemotaxis, haptotaxis, contact guidance, contact inhibition of locomotion (CIL), and cell–cell adhesion (Jotereau and Le Douarin, 1982; Hernandez-Fleming et al., 2017; Carter, 1965; de la Loza et al., 2017; Laumonnerie et al., 2015; Kridsada et al., 2018; Abercrombie and Heaysman, 1954; Carmona-Fontaine et al., 2008; Villar-Cerviño et al., 2013; Davis et al., 2015; Takeichi, 2014; Mayor and Etienne-Manneville, 2016; Scarpa and Mayor, 2016; Cousin, 2017). Migratory behavior of cells may be regulated by combinations of these guidance cues.

The axial skeleton of the trunk comprises a series of metamerically arranged vertebrae. The rib is such a characteristic thoracic structure that distinguishes the thorax from other regions of the axial skeleton in birds and mammals. The axial skeleton is derived from somites. Although thoracic somites have the potency to form ribs (Kieny et al., 1972), its exertion depends on the neighboring tissues around somites. In birds, a rib is composed of three compartments, viz., proximal rib, vertebro-distal rib, and sterno-distal rib, according to developmental dependencies of the adjacent tissues (Aoyama et al., 2005). The proximal rib is derived from a caudal half of somites under the influence of the ventral neural tube and notochord; the distal rib is derived from a caudal and rostral half of two adjacent somites under the influence of the surface ectoderm. Furthermore, the sterno-distal rib develops in relation to penetration into the somatic lateral plate mesoderm (LP) (Kato and Aoyama, 1998; Nowicki and Burke, 2000; Aoyama and Asamoto, 2000; Huang et al., 2000; Sudo et al., 2001; Aoyama et al., 2005).

It has been reported that interaction between thoracic somites and thoracic LP is important for the development of the sterno-distal rib.

* Corresponding author at: Department of Medical Science and Technology, Faculty of Health Sciences, Hiroshima International University, 555-36 Kurosegakuendai, Higashihiroshima City, Hiroshima 739-2695, Japan.
E-mail address: h-aoyama@hirokoku-u.ac.jp (H. Aoyama).

https://doi.org/10.1016/j.mod.2019.103568
Received 13 January 2019; Received in revised form 22 July 2019; Accepted 30 August 2019
Available online 04 September 2019
0925-4773/

When the thoracic segmental plate is ectopically transplanted into the cervical region, the ribs derived from the explants are shorter than normal ribs (Kieny et al., 1972; Shearman and Burke, 2009). A blockage between thoracic somites and LP causes the absence of sterno-distal ribs. Liem and Aoyama (2009) reported that when LP of the limb-forming region is transplanted into the thoracic region, sterno-distal ribs are truncated or absent with an ectopically formed wing or leg. Further, when the thoracic segmental plate is transplanted into the lumbosacral region, the grafted mesoderm forms ectopic ribs that have been much shorter than normal ribs (our unpublished data). Thus, somite and lateral plate interact differentially along rostro-caudal axis, which might support region specific rib-genesis. Although tissue-to-tissue interaction could be based on cell-to-cell interaction, it is difficult to analyze the intercellular interaction in a developing embryo.

Here, we established an in vitro co-culture system to investigate intercellular interaction between a somite cell and a LP cell. We found that thoracic somite cells change their direction of migration after contact with lumbar LP (LP-lu) cells but not after contact with thoracic LP (LP-th) cells.

2. Results

2.1. Co-culture experiment on a two-dimensional (2D) substrate: Behavior of thoracic somite cells on contact with thoracic somatic lateral plate (LP-th) or lumbar somatic lateral plate (LP-lu) cells

To investigate an interaction between somite cells and LP cells, somites and LP were isolated and were co-cultured in a liquid culture medium in a conventional glass base dish. The co-cultured tissues were as follows: thoracic somites (24th–25th somites) at HH-stage 16 (Hamburger and Hamilton, 1951) with LP-th (LP at 23rd–25th somite level) at HH-stage 16 and thoracic somites (21st–22nd somites) at HH-stage 15 with LP-lu (LP at 30th–31st somite level) at HH-stage 19 (Fig. 1A). The somite cell appeared to tend to change the direction of migration by contact with LP-lu cells, while it did not by contact with LP-th cells (Fig. 1B and C). This finding suggests that the thoracic somite cells have affinity with the thoracic LP, but are repellent to the lumbar LP. Although further quantitative analysis was needed, it was difficult in this assay because the cells migrated in various directions with changing migration speed. Moreover, a cell may successively or simultaneously contact several cells.

Therefore, we performed another assay on a one-dimensional (1D) substrate wherein the cells migrated along narrow paths.

2.2. Co-culture experiment on a 1D substrate: Thoracic or lumbar somite derivatives with LP-th or LP-lu cells

Pieces of sclerotome (SC), dermomyotome (DM) and LP were isolated from chick embryos (Fig. 2). We co-cultured SC or DM with LP on CytoGraph in which the cytophilic area is restricted (10-μm wide paths) (Fig. 3A). The cells migrated away from the explants on the cytophilic paths and made contact with the cell migrating from the opposite side after 12–18 h (Fig. 3B and C). The migrating cell had to move either forward or backward because it was confined to move on a narrow cytophilic path. The velocity of a cell represents both the direction and speed of cell migration, i.e., positive and negative velocity values indicate that the cell migrated forward and backward, respectively. We observed various patterns of migration. For example, a cell continuously migrated forward by pushing aside other cells, a cell changed its direction of migration to backward, and a cell almost stopped migrating on contact. To determine the effect of intercellular interaction between somite and LP cells on contact, we tracked the points of leading and trailing edges of the cells (Fig. 3D) using consecutive images and calculated the migration velocity (μm/min). Due to variation among CytoGraphs, the cells that migrated out of the cytophilic area in some experiments were discarded. Only the experimental results of cell migration on a narrow cytophilic path were accepted, and the experiment was repeated up to 11 cases. In Fig. 4, each line represents a cell whose leading and trailing edges (Fig. 3D) were tracked; the lines show migration 60 min before and after contact with co-cultured cells.

2.3. Specific gene expression of explants from embryos

To confirm that the isolated somite and LP cells kept their character during the culture, the isolated tissues were examined for their specificity by assaying specific gene expression (Fig. 5). Immediately after the isolation, the thoracic SC (SC-th), thoracic DM (DM-th), thoracic LP (LP-th) strongly expressed *Foxc2*, *Pax3* and *Prx1*, respectively, which were reported to be a specific marker of each embryonic tissue (Sudo et al., 2001; Williams and Ordahl, 1997; Kuratani et al., 1993; Funayama et al., 1999). After the culture for one day, SC-th, DM-th and LP-th were found to express their specific markers. The specific gene expression suggests that the explants retained their specificity after one day culture in vitro.

2.4. Behavior of thoracic sclerotome (SC-th) cells co-cultured with LP-th or LP-lu cells

When SC-th cells were co-cultured with LP-th or LP-lu cells, before contact, their average migrating velocity at the leading edge was

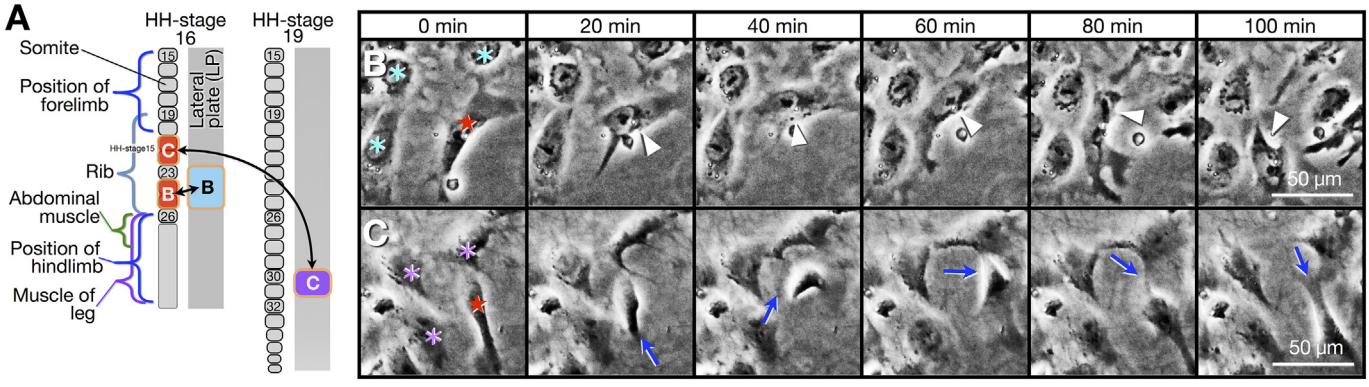

Fig. 1. Behavior of somite cell before and after contacting lateral plate cells on a conventional two-dimensional substrate. (A) Schematic illustration of excised tissue and developmental fate along the rostrocaudal axis. B and C in panel A indicate the explants for panels B and C. (B and C) Phase-contrast consecutive images. (B) A thoracic somite cell (red star) did not change the direction of migration (white arrowhead) for several minutes after contact with LP-th cells (blue asterisk). (C) A thoracic somite cell (red star) changed the direction of migration (blue arrow) immediately after contact with LP-lu cells (magenta asterisk). Abbreviations: LP, somatic lateral plate; -th, thoracic; -lu, lumbar.

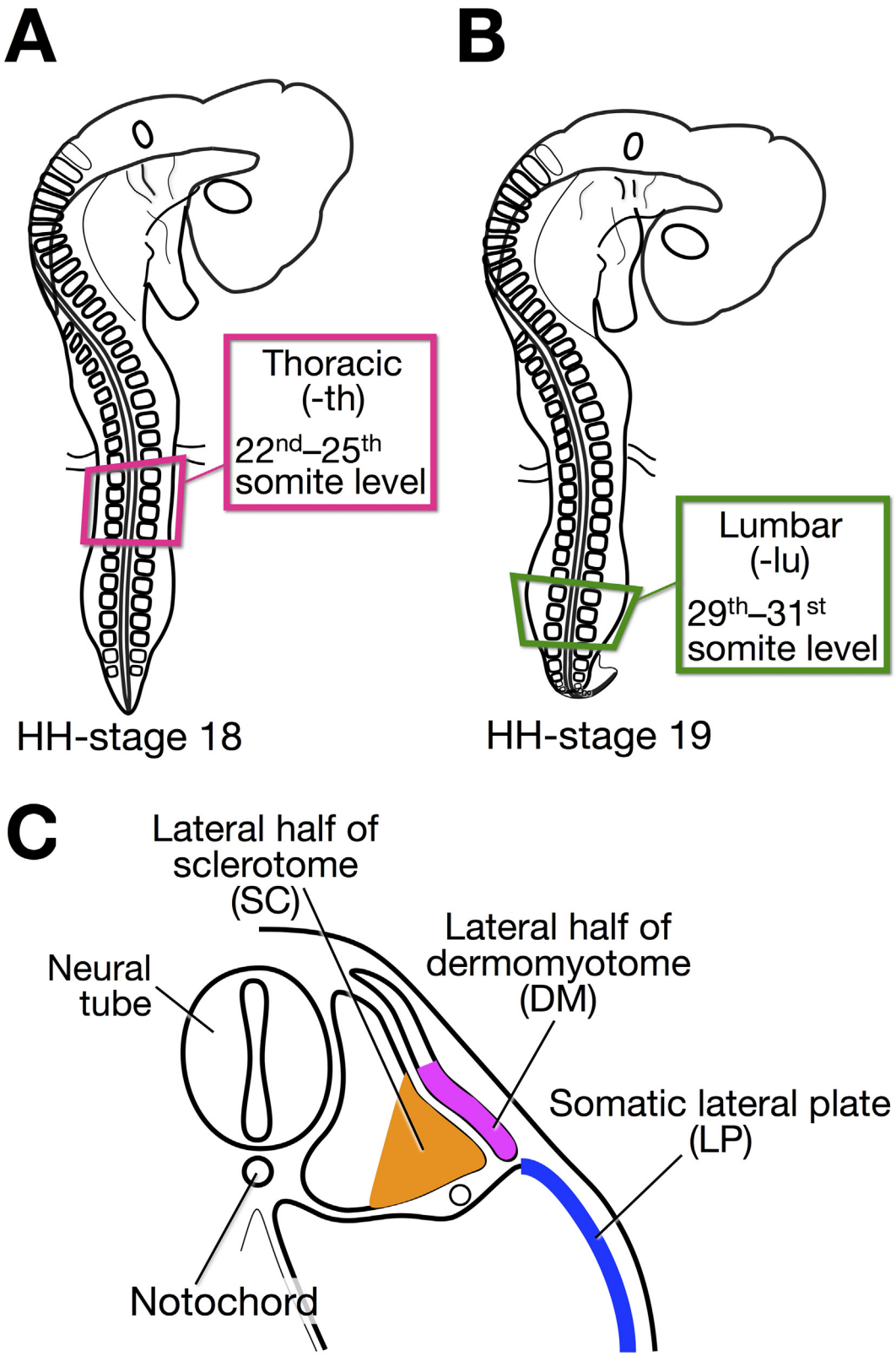

Fig. 2. Diagram illustrating the location of excision. (A) Schematic illustration of embryos showing the location of excision. The thoracic tissues were excised at 22nd–25th somite level from embryos. (B) The lumbar tissues were excised at 29th–31st somite level from embryos. (C) Schematic illustration of transverse section of an embryo showing excised tissues, lateral half of sclerotome (SC), lateral half of dermomyotome (DM), and somatic lateral plate (LP).

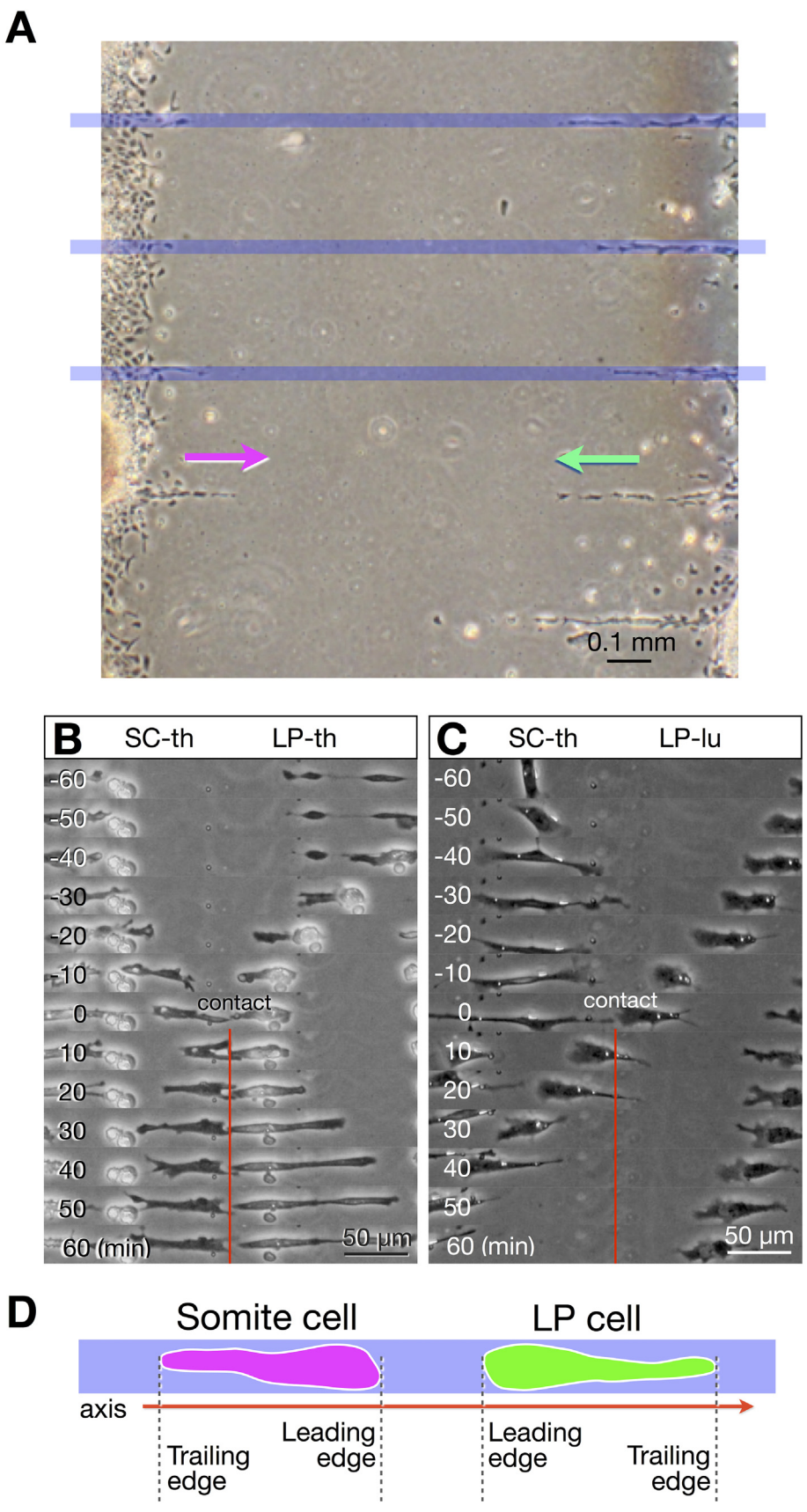

Fig. 3. Cell migration on a one-dimensional substrate, the CytoGraph. (A) SC and LP fragments were isolated from chick embryos and explanted on the opposite side of the cytophilic pathways [upper three pathways in (A) indicated with blue lines], which were 10-μm wide with 300-μm cytophobic intervals. SC (magenta arrow) and LP cells (green arrow) migrated away from the explants and continued to migrate along the cytophilic pathways. (B and C) Consecutive photos of SC cells and LP cells migrating from the opposite ends of the cytophilic pathways. Photos were captured every 10 min for 60 min before (negative values) and after (positive values) cells made contact with each other. (B) SC-th and LP-th cells were co-cultured. SC-th cells stopped migration after contact with LP-th cells. (C) SC-th and LP-lu cells were co-cultured. SC-th cells migrated in the reverse direction after contact with LP-lu cells. (D) Definition of the leading and the trailing edge in the migrating cell. Abbreviations: SC, sclerotome; LP, somatic lateral plate; -th, thoracic; -lu, lumbar.

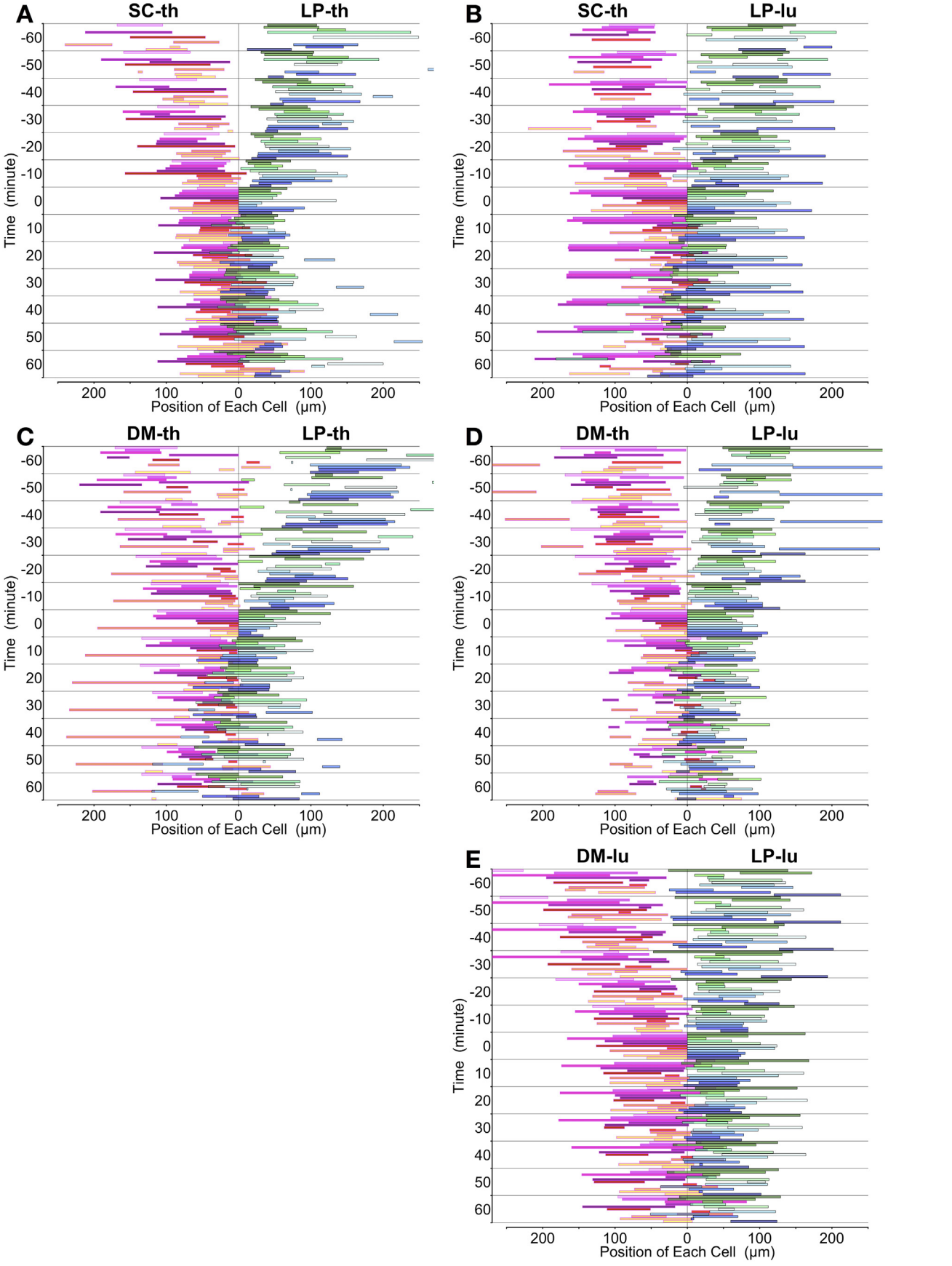

(caption on next page)

Fig. 4. Position of two co-cultured cells migrating from the opposite side on a one-dimensional substrate. Each line represents a cell with leading and trailing edges (x-axis), which were determined according to the contact point. Lines of the same color represent the same cell in each figure. (A) SC-th and LP-th cells were co-cultured five times (N = 5), and 11 pairs of cells were recorded (n = 11). (B) SC-th and LP-lu cells (N = 5; n = 11). (C) DM-th and LP-th cells (N = 3; n = 11). (D) DM-th and LP-lu cells (N = 5; n = 11). (E) DM-lu and LP-lu cells (N = 5; n = 11). We eliminated the data from cells when their trailing edge was too obscure to determine. Abbreviations: SC, sclerotome; LP, somatic lateral plate; DM, dermomyotome; -th, thoracic; -lu, lumbar.

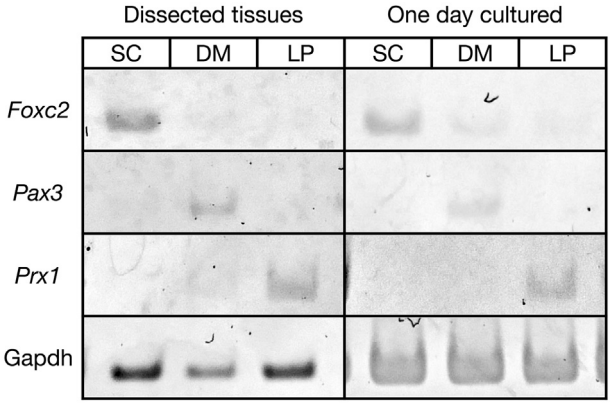

Fig. 5. Specific gene expression of the explants from chick embryos. Specific gene expression of explants shown by RT-PCR, immediately after dissection (left column) and after one day culture (right column). For analysis of tissues just after the dissection, sclerotome (SC), dermomyotome (DM), and somatic lateral plate (LP) at 21st–23rd somite level were dissected from 7 chick embryos at HH-stage 17–18 (30–32 somite stage). For one-day culture, SC, DM, and LP were dissected from HH-stage 17–19 (29–39 somite stage) 71 chick embryos. RT-PCR analysis was performed to detect the expression of the sclerotomal marker *Foxc2*, the dermomyotome marker *Pax3*, the somatic LP marker *Prx1*, and the internal control Gapdh. Each explant expressed its specific marker both before and after the culture. Abbreviations: SC, sclerotome; DM, dermomyotome; LP, somatic lateral plate.

1.36 ± 0.23 μm/min (n = 11) and 1.56 ± 0.37 μm/min (n = 11), respectively (Fig. 6A). Before contact, there was no significant difference in the migration velocity. However, after contact with LP-th or LP-lu cells, the velocity decreased to 0.46 ± 0.15 μm/min (n = 11) and − 0.55 ± 0.23 μm/min (n = 11), respectively, wherein the negative value represents backward migration (Fig. 6A). Although contact with LP-th cells decreased the velocity of SC-th cell migration by 34%, SC-th cell continuously migrated forward. However, contact with LP-lu cells altered SC-th cell movement to the opposite direction.

Cells on the CytoGraph did not always migrate at a constant velocity, and the velocity varied from cell to cell. Fig. 6B and C show the relative frequency of cells (percentage) migrating at a certain velocity. Here, the velocity was represented as that of the leading edge. Velocity data were classified into eight classes at intervals of 1 μm/min (Fig. 6B and C). In Fig. 6, bar graph on the right side represents forward movement and that on the left side represents backward movement.

Based on these data, we analyzed the migratory behavior of somite cells before and after contact with LP cells.

Most SC-th cells (66.7%) continuously migrated forward after contact with LP-th cells, although their speed became relatively low (Fig. 6B). Thirty minutes before contact, 24.1% SC-th cells migrated at the speed of 0–1 μm/min, whereas the percentage of cells increased to 48.5% after contact (Fig. 6B). In contrast, most SC-th cells (66.7%) migrated backward after contact with LP-lu cells (Fig. 6C). Moreover, > 10% of the cells migrated backward at a velocity of > 3 μm/min 30–60 min after contact (Fig. 6C). Thus, after contacting LP cells, the direction of migration of SC-th cells depended on the rostro-caudal level of LP cells.

2.5. Behavior of LP-th and LP-lu cells co-cultured with SC-th

Most LP-th cells migrated forward (88.7%) at a high speed (average velocity of 1.58 ± 0.39 μm/min; n = 11) before contact with SC-th cells (Fig. 6D and E). Fig. 6E and F show the proportions of cells migrating at different velocities. To calculate the velocity of a cell, the movement of its leading edge was measured. Within 30 min after contact, although LP-th cells still predominantly migrated forward (60.6%, Fig. 6E), > 30% of LP-th cells changed their direction of migration. This tendency was more conspicuous 30–60 min after contact. However, the velocity of LP-lu cells did not significantly change before and after contact with SC-th cells (Fig. 6D and F).

2.6. Behavior of thoracic DM (DM-th) cells co-cultured with LP-th or LP-lu cells

Most DM-th cells migrated forward 30 min before contact with LP-th cells (78.8%; average velocity of 1.02 ± 0.35 μm/min; n = 11), whereas most DM-th cells migrated in the opposite direction after contact (75.8%, average velocity of −0.56 ± 0.25 μm/min; n = 11) (Fig. 7A and B). We observed that DM-th cells with their leading edge in contact with the leading edge of LP-th cells elongated backward in six of 11 cases (Fig. 4C). After contact with LP-th cells, DM-th cells exhibited stagnation in its leading edge and extension of the trailing edge, suggesting that these cells were to migrate backward but were unable to move due to cell–cell adhesion.

Within 30 min before contact with LP-lu cells, > 70% of DM-th cells migrated forward (average velocity of 1.37 ± 0.40 μm/min; n = 11), whereas within 30 min after contact, approximately 50% of the cells migrated backward (average velocity of −0.59 ± 0.33 μm/min; n = 11) (Fig. 7A and C). In particular, > 20% of cells migrated backward at a velocity of > 2 μm/min. On contact with LP-lu cells, DM-th cells exhibited a sudden regression in the leading edge and backward extension of the trailing edge in five of 11 cases (Fig. 4D).

2.7. Behavior of LP-th and LP-lu cells co-cultured with DM-th cells

Before contact with DM-th cells, LP-th cells migrated forward at a high speed (average velocity of 1.91 ± 0.26 μm/min; n = 11), whereas their average velocity decreased significantly to 0.43 ± 0.25 μm/min (n = 11) after contact (Fig. 7D). This was primarily because of the decrease in cell population migrating at a velocity of > 3 μm/min and increase in cells migrating backward (Fig. 7E). Nevertheless, LP-th cells predominantly and continuously migrated forward after contact with DM-th cells.

LP-lu cells migrated forward at a high speed (average velocity of 1.20 ± 0.29 μm/min; n = 11) before contact with DM-th cells (Fig. 7D). After contact with DM-th cells, the average velocity of LP-lu cell leading edges was −0.03 ± 0.15 μm/min (n = 11) (Fig. 7D). These cells did not cease to migrate, but approximately half of the cells began to migrate backward (Fig. 7F). Leading edges migrating forward at a velocity of > 2 μm/min decreased, whereas leading edges of cells migrating backward at low speed (< 1 μm/min) increased on contact with DM-th cells (Fig. 7F).

2.8. Behavior of lumbar DM (DM-lu) cells co-cultured with LP-lu cells

DM-lu cells migrated forward at a high speed (average velocity of 1.46 ± 0.29 μm/min; n = 11) before contact with LP-lu cells (Fig. 8A). Thirty minutes before contact with LP-lu cells, more than half of DM-lu cells migrated forward at a velocity of > 2 μm/min, whereas approximately 50% of cells migrated backward after contact (Fig. 8B). Only in

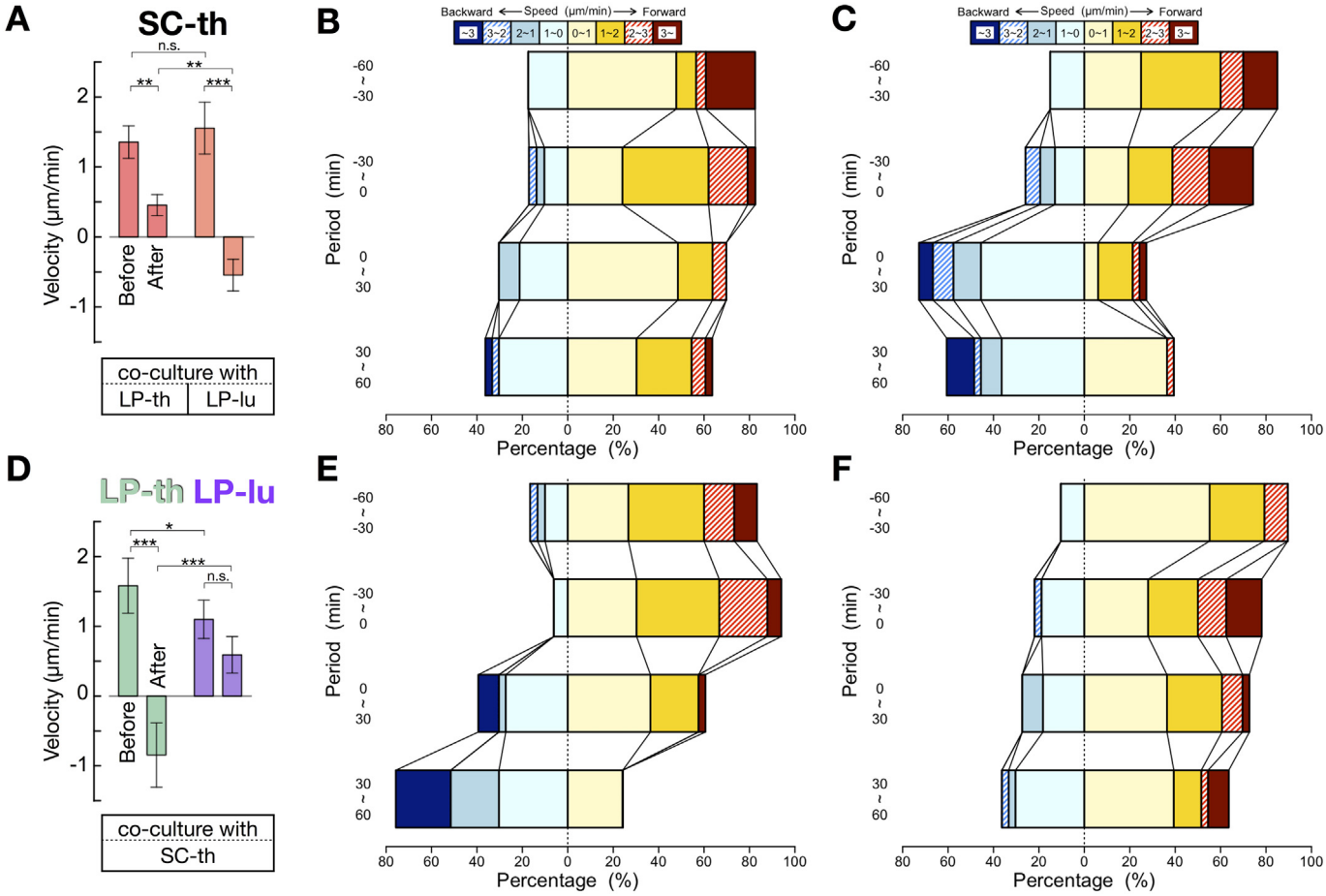

Fig. 6. Change in the migration velocity of SC-th and LP-th or LP-lu cells before and after contact with each other on the one-dimensional substrate. Velocity was represented as that of the leading edge of migrating cells and calculated every 10 min. (A and D) Changes in average velocity of the cell 60 min before and after contact with its counterpart. (B, C, E, F) Horizontal stacked bar charts represent the percentage of cumulative cell numbers migrating at the velocity indicated above the chart. (A) SC-th cells continued to migrate at a lower velocity after contact with LP-th cells (n = 11) but changed the direction of migration after contact with LP-lu cells (n = 11). (B) Forward migrating SC-th cells decreased slightly to approximately 60% after contact with LP-th cells. (C) After contact with LP-lu cells, backward migration of SC-th cells increased notably. (D) LP-th cells changed the direction of migration after contact with SC-th cells, whereas LP-lu cells continued to migrate after contact with SC-th cells. (E) After contact with SC-th cells, backward migration of LP-th cells increased notably. (F) Forward migration of LP-lu cells decreased slightly after contact with SC-th cells. Abbreviations: SC, sclerotome; LP, somatic lateral plate; -th, thoracic; -lu, lumbar; n.s., no significant difference; $^{*}P < 0.05$; $^{**}P < 0.01$; $^{***}P < 0.001$. Data are represented as means ± SE.

the combination of this co-culture, the leading edges of DM-lu cells migrated at very low speed after contact (average velocity of 0.14 ± 0.20 μm/min; n = 11) (Figs. 4E, 8B).

2.9. Behavior of LP-lu cells co-cultured with DM-lu cells

LP-lu cells migrated forward (average velocity of 0.49 ± 0.23 μm/min; n = 11) before contact with DM-lu cells (Fig. 8C). Approximately 70% of LP-lu cells migrated forward within 30 min before contact (Fig. 8D). After contact with DM-lu cells, approximately 70% of LP-lu cells migrated backward, which decreased to approximately 40% at 30 min after contact (Fig. 8D). LP-lu cells migrated backward, but by contact with another LP cell behind it, the cells changed the direction of migration again in seven of 11 cases.

2.10. Behavior of SC-lu cells

We tried to perform experiments using SC-lu cells. However, SC-lu cells hardly migrated to make contact with other cells (data not shown).

2.11. Alteration in cell size before and after contact with LP cells

We examined change in the cell length after the contact with co-cultured cells. Fig. 9 shows standardized cell lengths that are presented as percentages of cell length after the contact. The average cell length calculated from measurements taken every 10 min for 60 min before contact was considered as 100%. Cell length was determined between the leading and trailing edges of cells. After contact with LP-lu cells, the length of both SC-th and DM-th cells reduced remarkably. On contact with LP-th cells, the length of SC-th and DM-th cells did not virtually change before and after contact. The length of DM-lu cells did not change either on contact with LP-lu cells. The length of LP-lu cell was not different significantly after contact among any combination in this experiment (data not shown).

2.12. Grouping velocity distribution patterns by hierarchical clustering analysis

As shown in Figs. 6–8, somite and LP cells migrated at various velocity distribution patterns based on the combination of their co-culture (Figs. 6B, C, E, F; 7B, C, E, F; 8B, D). Clustering analysis revealed that velocity distribution patterns were divided into three groups (Fig. 10A),

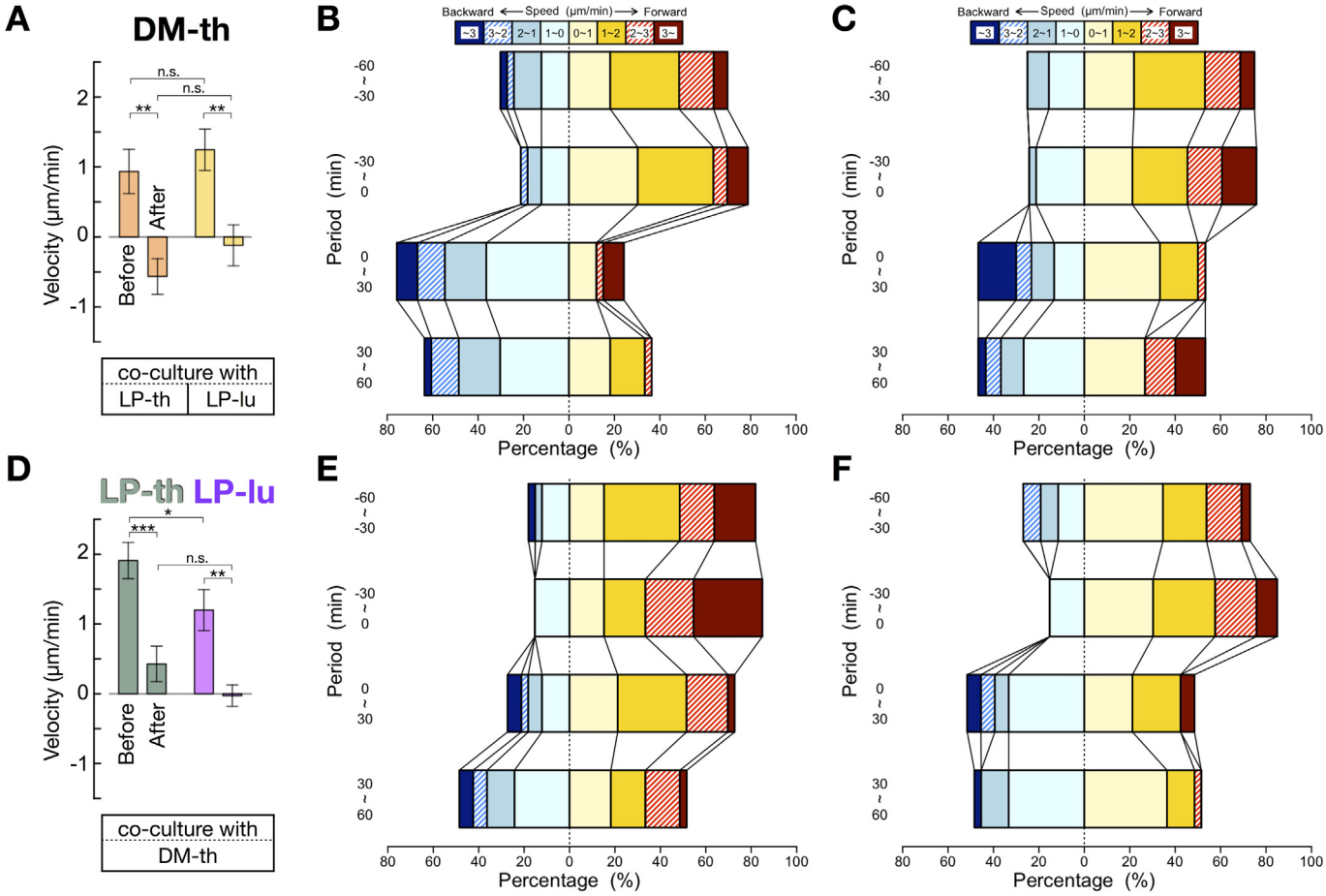

Fig. 7. Change in migration velocity of DM-th and LP-th or LP-lu cells before and after contact with each other on the one-dimensional substrate. The velocity was represented as that of the leading edge of migrating cells and was calculated every 10 min. (A and D) Changes in average velocity of the cell 60 min before and after contact with its counterpart. (B, C, E, F) Horizontal stacked bar charts represent the percentage of cumulative cell numbers migrating at the velocity indicated above the chart. (A) DM-th cells changed the direction of migration after contact with LP-th cells (n = 11), whereas the velocity of migration appeared to be very low after contact with LP-lu cells (n = 10). (B) Most DM-th cells changed the migration direction to backward after contact with LP-th cells. (C) More than half DM-th cells continued forward migration, whereas a certain number of cells began backward migration at a relatively high speed after contact with LP-lu cells. (D) LP-th cells continued to migrate at a lower velocity after contact with DM-th cells, whereas LP-lu cells appeared to cease migration after contact with DM-th cells. (E) After contact with DM-th cells, forward migration of LP-th cells decreased gradually. Just after contact, they continued to migrate forward (0–30 min). After 30–60 min, some cells began to migrate backward. (F) Forward migration of LP-lu cells decreased to approximately 50% after contact with DM-th cells, which resulted in very low average velocity as shown in D. Abbreviations: DM, dermomyotome; LP, somatic lateral plate; -th, thoracic; -lu, lumbar; n.s., no significant difference; $^{*}P < 0.05$; $^{**}P < 0.01$; $^{***}P < 0.001$. Data are represented as means ± SE.

and distinctive features were observed in all velocity distribution patterns (Fig. 10B). CL1 (cluster one) was characterized by forward migration at > 1 μm/min. In CL2, the cells migrated forward at low velocity. In CL3, the proportion of backward migration was high.

SC and DM cells predominantly migrated forward before contact (Fig. 10C, 2nd line; CL1). The direction of migration of somite cells changed to backward after contact with LP cells (Fig. 10C, 3rd, 5th, 7th and 9th columns; CL3), except for SC-th cells that continuously migrated forward (CL2) after contact with LP-th cells (Fig. 10C, 1st column).

Although migration of DM-th cells after contact with LP-lu cells was grouped under CL2 (Fig. 10, 7th column), 16.7% of DM-th cells migrated backward at a velocity of > 3 μm/min (Fig. 7C), indicating that a considerable number of DM-th cells migrated backward, unlike other cells grouped in CL2 (Fig. 10A, heatmap).

On contact with SC-th cells, LP-th cells changed the direction of migration (Fig. 10C, 2nd column). Before contact, LP-th cells migrated forward at a high velocity (CL1), but the cells migrated backward after contact (CL3). On the contrary, LP-lu cells always migrated forward (CL1 and CL2) before and after contact with SC-th cells (Fig. 10C, 4th column). After contact with DM-lu cells, LP-lu cells transiently changed the direction of migration to backward (CL3) and then again to forward at low velocity (CL2) (Fig. 10C, 10th column).

3. Discussion

3.1. In vitro system for examining behavior of somitic cells

A major portion of the axial skeleton of vertebrates is derived from somites. They form various bones along the rostro-caudal axis, from the occipital bone to the coccygeal bone. Of these somites, thoracic somites particularly form long ribs in addition to the thoracic vertebrae. As shown by Kieny et al. (1972), although thoracic somites specifically form the ribs, their length depends on the neighboring conditions. When the thoracic segmental plate is ectopically transplanted into the cervical region, the transplants form vertebral ribs but no sternal ribs.

For rib formation, thoracic somite cells penetrate into the somatic lateral plate mesoderm. When the thoracic somite mesoderm is transplanted into the lumbar region, it does not penetrate into the lumbar somatic mesoderm and forms short ribs (Matsumori et al., unpublished data). We hypothesized that the intercellular interaction between somite and LP cells could control cell behavior to form the axial skeleton.

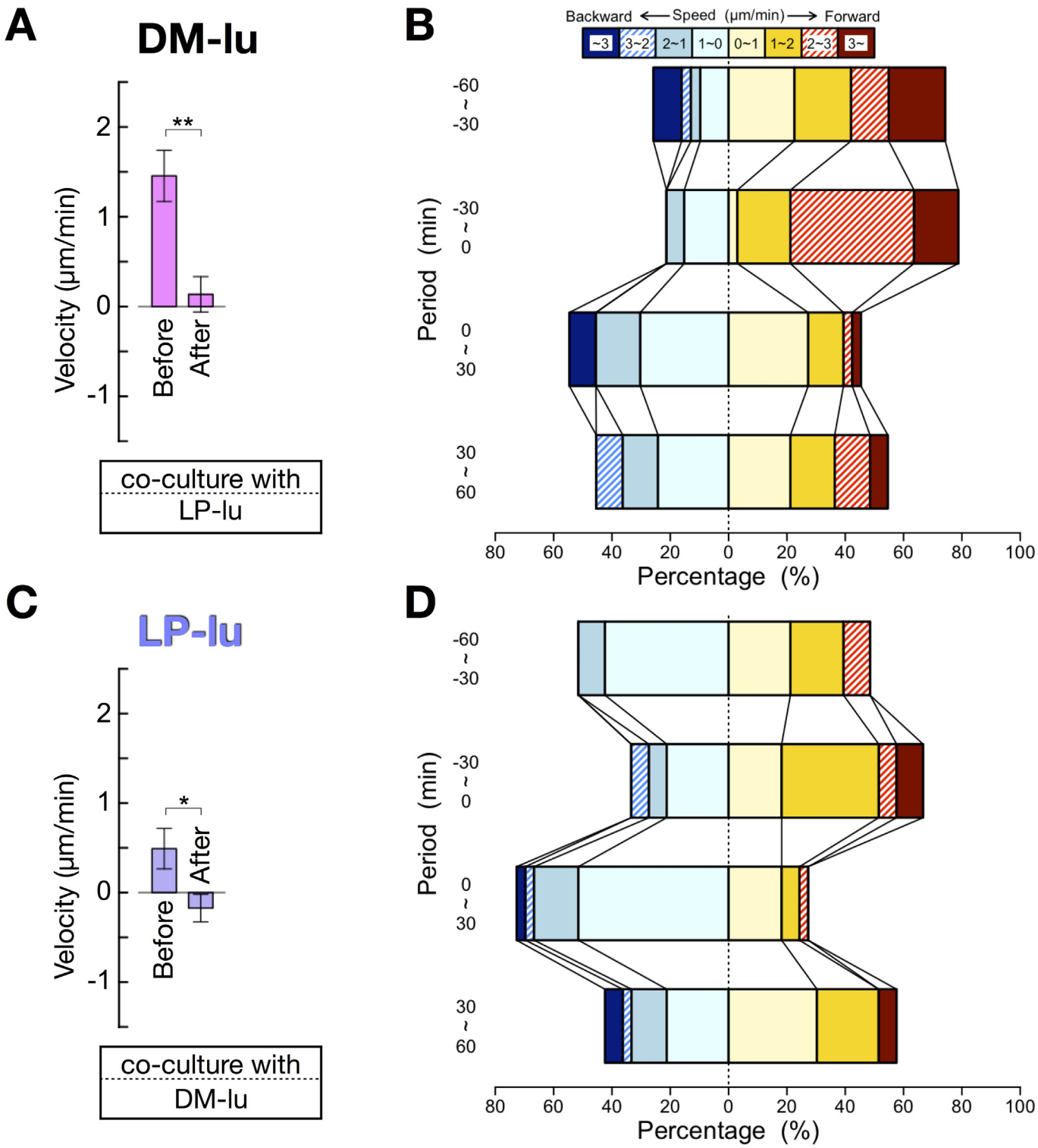

Fig. 8. Change in migration velocity of DM-lu and LP-lu cells before and after contact with each other on the one-dimensional substrate. Velocity was represented as that of the leading edge of migrating cells and calculated every 10 min. (A and C) Change in the average velocity of cells 60 min before and after contact with its counterpart. (B and D) Horizontal stacked bar charts represent the percentage of cumulative cell numbers migrating at the velocity indicated above the chart. (A) DM-lu cells appeared to continue migration at a lower velocity after contact with LP-lu cells (n = 11). (B) Just after contact with LP-lu cells, a certain number of DM-lu cells began to migrate backward at a relatively high speed (> 3 μm/min). The percentage of DM-lu cells migrating forward decreased once to approximately 50% 0–30 min after contact, and then it increased slightly in the following 30–60 min. (C) LP-lu cells changed the direction of migration after contact with DM-lu cells (n = 11). (D) The percentage of LP-lu cells migrating forward decreased once to approximately 30% 0–30 min after contact with DM-lu cells, and then it increased to approximately 60% in the following 30–60 min after contact. Just after contact (0–30 min), > 70% of cells migrated backward, although most cells migrated at a relatively low velocity (0–1 μm/min). Abbreviations: DM, dermomyotome; LP, somatic lateral plate; -th, thoracic; -lu, lumbar; n.s., no significant difference; *$P < 0.05$; **$P < 0.01$; ***$P < 0.001$. Data are represented as means ± SE.

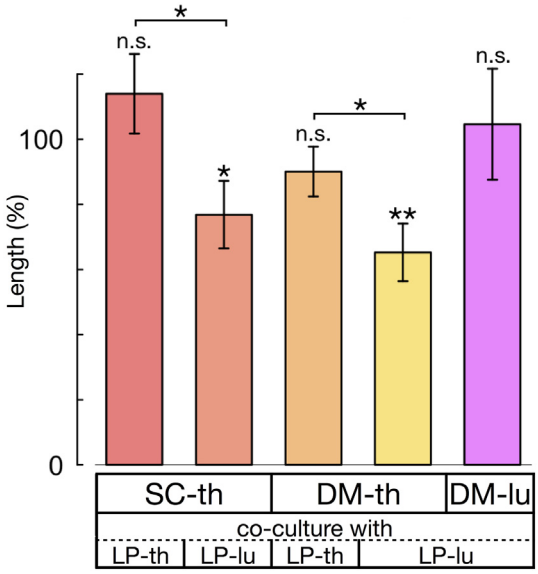

Fig. 9. Standardized cell lengths that are presented as percentages of cell length after the contact. Cell length was measured from the leading edge to the trailing edge. To calculate the ratio of cell length, each cell length after the contact was divided by the average cell length of the cell before contact. The ratio of length of both SC-th and DM-th cells was significantly shorter when they made contact with LP-lu cells than that when they made contact with LP-th cells. Abbreviation; -th, thoracic; -lu, lumbar; SC, sclerotome; DM, dermomyotome; LP, lateral plate. Error bars denote SE. DM-th cells made contact with LP-lu cells, n = 10. n = 11, except for when DM-th cells made contact with LP-lu cells. n.s., no significant difference; $*P < 0.05$; $**P < 0.01$.

Here, we present the migratory behavior of somite and somatic LP cells in an in vitro co-culture system and showed that SC-th cells tended to continuously migrate forward after contact with LP-th cells, whereas they migrated in the reverse direction after contact with LP-lu cells.

Embryonic cells isolated in vitro may change their developmental fate, which would misinterpret our findings. In fact, the epithelial somite develops depending on its surrounding tissues. The surface ectoderm induces the DM, and the notochord and floor plate induces the SC. Even if each somitic primordium is combined with an ectopic tissue, it develops according to the tissue in contact (Aoyama and Asamoto, 1988; Ordahl and Le Douarin, 1992; Christ et al., 1992; Pourquié et al., 1993; Aoyama, 1993; Christ and Ordahl, 1995; Williams and Ordahl, 1997; Dockter and Ordahl, 2000; Monsoro-Burq, 2005). However, as we have shown, the caudal third somite (stage III somite) begins to differentiate and at least some part of it cannot change its fate after being rotated dorsoventrally (Aoyama and Asamoto, 1988). The presumptive dermomyotomal region and a part of the presumptive sclerotomal region of the somite differentiate along their original fate under heterotopic circumstances. Furthermore, except for stage I–III somites, isolated somites differentiate into cartilage tissue and muscle fibers without induction of other tissues in vitro (Ellison et al., 1969a, 1969b; Kenny-Mobbs and Thorogood, 1987; Buffinger and Stockdale, 1994; Stern and Hauschka, 1995). We did not use stage I–III somites in the present study. Thus, the somite cells that we investigated in vitro were considered to retain their fate and represent their behavior in vivo. Further, we have shown that the cultured cells expressed their specific gene for one day (Fig. 3), suggesting that they retained their specificity during the culture. Nevertheless, since we examined gene expression in an isolated mass of cells instead of in a single cell that contacted another cell, it is not clear which cell has retained the character of the whole mass of cells.

In the present study, we primarily used the 1D migratory system instead of the 2D system because of simplicity of analysis of cell migratory behavior. It has been reported that there is no considerable difference in neural crest cell behavior and migratory abilities between the 1D and 2D systems, although speed and directionality were slightly less in the 1D system than those in the 2D system (Scarpa et al., 2013, 2016). The velocity of SC-th cells co-cultured with LP-th cells was 1.36 ± 0.23 μm/min (n = 11) (Fig. 6A), of DM-th cells co-cultured with LP-th cells was 0.94 ± 0.32 μm/min (n = 11) (Fig. 7A), and of LP-th cells co-cultured with SC-th cells was 1.58 ± 0.39 μm/min (n = 11) (Fig. 6D). Our results almost agree with the velocities of SC (1.095 μm/min), DM (1.085 μm/min), and LP (1.925 μm/min) cells reported by Bellairs et al. (1980) at the interval of 12 s.

3.2. Reaction of cells after contact with other cells

We observed two types of reactions of cells upon the cell-cell contact, a) keeping forward migration or b) turning to backward. The change in direction of cell migration could be because of three mechanisms as given below:

1) The contact activates signaling to change the migration direction of the cell.
2) The contact activates signaling to stop migration, which is known as contact inhibition of locomotion. When the cell re-starts migration, it finds a free space to migrate opposite the contacted cell.
3) Even if a cell has a capacity to migrate forward, another cell may push the cell and/or block its forward migration. In such a case, the leading edge would retract, while the trailing edge would keep its position or migrate forward, and then, the cells would shorten to round up.

In the present study, the behavior of the cells after the contact was by 1) or 2). Although we could not distinguish between 1) and 2), both represent active reaction on the cell-cell contact. On the other hand, we found no cases of 3). Even though some cells shortened after the contact (Fig. 9), they did not round up but soon migrated backward.

Thus, the cells do not behave passively, but actively, on the contact with the other cells.

3.3. Behavior of sclerotome cells affected by cell-cell interaction in vitro

We found that SC-th cells changed the direction of migration just after contact with LP-lu cells, suggesting that the effect of intercellular interaction is not based on long-range mechanisms, such as chemotaxis, haptotaxis, or contact guidance, but on cell–cell contact. After contact with LP-th cells, SC-th cells, which form the rib anlagen, continued migrating in the same direction as that before contact (Fig. 10C, 1st column). However, after contact with LP-lu cells, SC-th cells migrated in the opposite direction (Fig. 10C, 3rd column) and the length of SC-th cells reduced (Fig. 9). It has been reported that contact inhibition results in restriction of the velocity of cells, changes the direction of cell migration (Abercrombie and Heaysman, 1954) and causes contraction (Abercrombie, 1970). A series of studies has reported that cell–cell contact affects the behavior of cells. Eph family ligands guide the migration of neural crest cells and motor axon from the neural tube (Wang and Anderson, 1997). Drosophila macrophages undergo contact repulsion and disperse laterally to form a “three-lined” organization pattern from a linear cellular array at the ventral midline (Stramer et al., 2010; Davis et al., 2012; Davis et al., 2015). Neural crest cells migrate in an N-cadherin/CIL-dependent mechanism (Erickson, 1985; Carmona-Fontaine et al., 2008; Theveneau et al., 2010; Scarpa et al., 2015). In these studies, the behaviors of cells were analyzed in vitro and were confirmed in vivo.

To form the ribs, SC-th cells start to migrate ventrolaterally while proliferating, and then penetrate into the somatopleure. The length of a rib could be determined by migrating speed and/or proliferating ratio. When SC-th cells contact LP-th cells, they continued to migrate forward at a velocity of 0.46 ± 0.15 μm/min (n = 11; Fig. 6A). After migrating

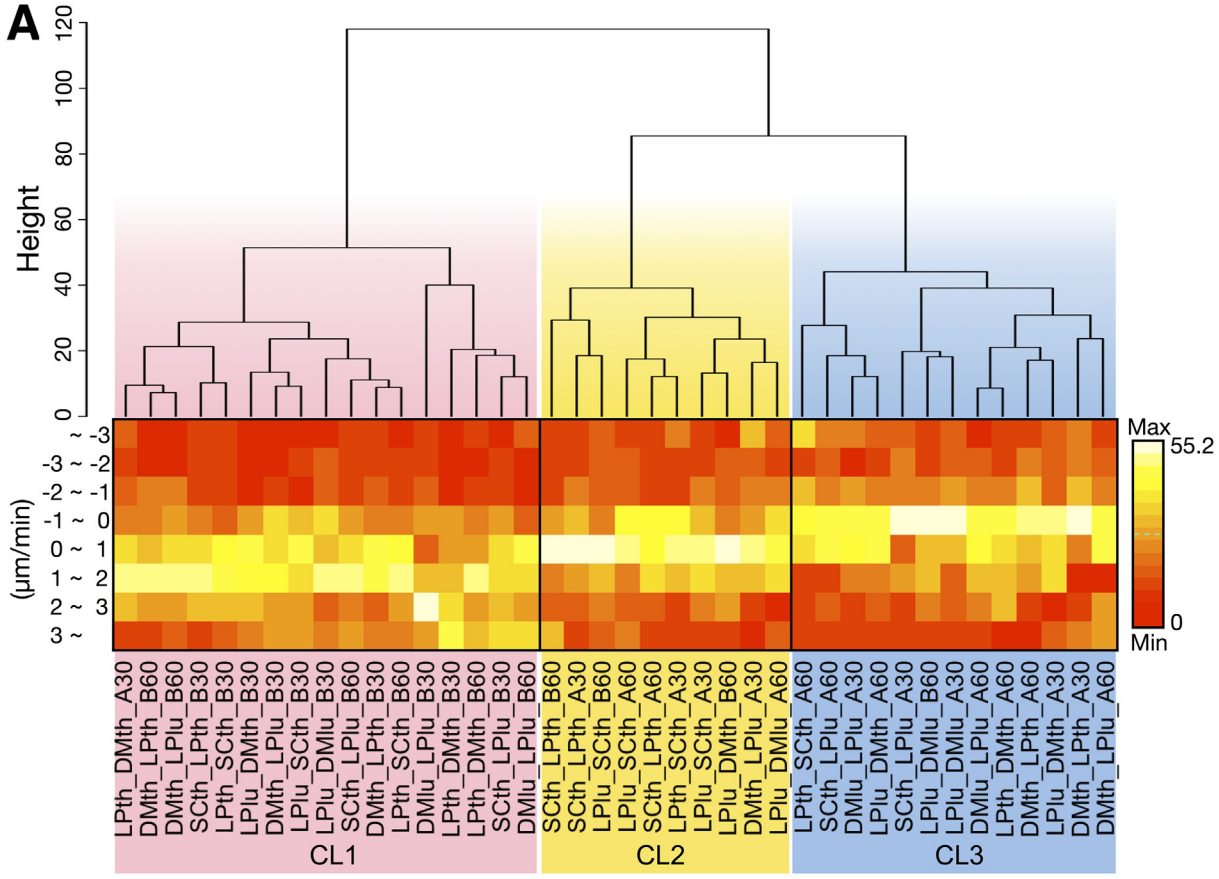

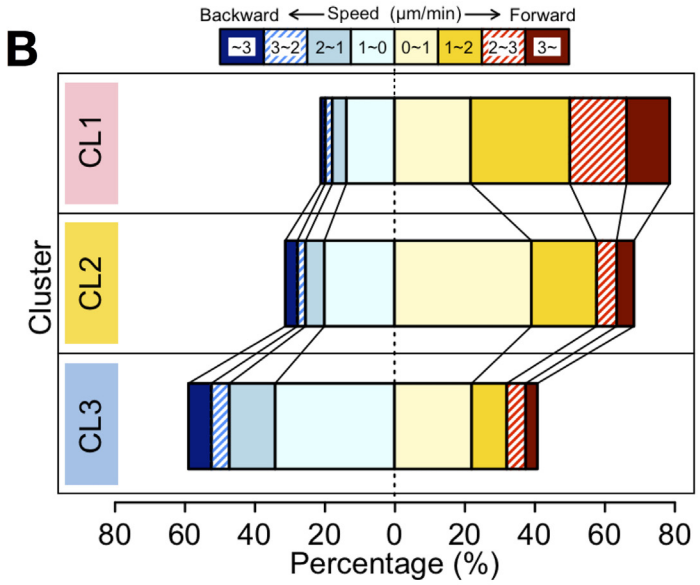

C

co-culture	SC-th vs. LP-th		SC-th vs. LP-lu		DM-th vs. LP-th		DM-th vs. LP-lu		DM-lu vs. LP-lu	
	SC-th	LP-th	SC-th	LP-lu	DM-th	LP-th	DM-th	LP-lu	DM-lu	LP-lu
Period (min) -60 ~ -30	CL2	CL1	CL1	CL2	CL1	CL1	CL1	CL2	CL1	CL3
-30 ~ 0	CL1	CL1	CL1	CL1	CL1	CL1	CL1	CL1	CL1	CL1
0 ~ 30	CL2	CL2	CL3	CL2	CL3	CL1	CL2	CL3	CL3	CL3
30 ~ 60	CL2	CL3	CL3	CL2	CL3	CL3	CL3	CL3	CL3	CL2

(caption on next page)

Fig. 10. Cluster analysis of migratory behavior. (A) Cluster dendrogram of velocity distribution of the cell. Height indicates criterion value in our agglomeration adapting the Ward's method. Heatmap represents the relative frequencies of cumulative cell numbers. White color indicates the maximum value. Clustering cells are indicated under the heatmap with co-cultured cells and with measured time period. (B) Difference in the velocity distribution pattern between clusters. In each cluster, we calculated the average of the relative frequencies of cells (percentage) migrating at each velocity indicated above the chart. (C) The time-course of changes in cell migration pattern are indicated by the cluster. Same clusters are indicated with the same background color. For example, the migratory behavior of SC-th cells co-cultured with LP-th cells always belonged to CL1 or CL2, whereas those co-cultured with LP-lu cells changed from CL1 to CL3 after contact with LP-lu cells. Abbreviation; SC, sclerotome; DM, dermomyotome; LP, lateral plate; th, thoracic; lu, lumbar; B60, before 60–30 min; B30, before 30–0 min; A30, after 0–30 min; A60, after 30–60 min.

for 7.5 days at this velocity, the migrated distance would be 4.97 mm, which is almost the same length as the 4th vertebral rib, 4.95 ± 0.18 mm (n = 10) at HH-stage 36 (approximately 10 days after incubation). Thus, migrating speed of the SC cells was in accordance with the length of the rib, suggesting that cell migration speed might be significant factor to determine the length of a rib. However, several issues remain to be elucidated. In this study, we could not distinguish sub-populations of SC cells. The migratory behavior of proximal rib anlagen and distal rib anlagen might be different, since the proximal rib is much shorter than the distal rib. Moreover, distal rib comprised of the vertebral and the sternal rib. The SC cells migrate as a compact population to form the vertebral rib, while they intermingle with the LP cells to form the sternal rib (Burke and Nowicki, 2003). The behavior of SC cells would be different among subpopulations. To elucidate the role of cell migration in rib formation, we have to compare migrating speed between cells in different subpopulations. Further, cell proliferation might be another important factor for morphogenesis, which we did not address in the present study.

On the other hand, SC-th cells reversed the direction of migration after contact with LP-lu cells (Fig. 10C, 3rd column). At 0.55 ± 0.23 μm/min (n = 11), SC-th cells migrated away from LP-lu cells after contact (Fig. 6A). This phenomenon may represent the somite cell behavior in vivo. Ectopic transplantation of leg somatopleural mesoderm in the thoracic region alters the fate of somite descendant cells and causes the loss of sterno-distal ribs. Furthermore, we found that thoracic somite cells did not enter into the tissue derived from the lumbar lateral plate when the thoracic somite mesoderm was ectopically transplanted in the lumbar region. In normal development, SC-th cells can contact LP-lu cells only at the thoraco–lumbar boundary. This repulsive nature of intercellular interaction observed in the present study would help to avoid malformation caused by penetration of rib-forming thoracic somite cells into the lumbar lateral plate by accident.

Burke and Nowicki (2003) proposed that the body wall should be classified into two categories, viz., primaxial and abaxial regions, according to the relationship between the somite and lateral plate mesoderm in the course of development. The domain comprising only somite cells is defined as the primaxial region, and the domain of the lateral plate with somite and lateral plate cells is defined as the abaxial region. They named the interface between the primaxial and the abaxial region as the lateral somitic frontier. At the thoracic level, the cluster of somite cell population elongates laterally into the lateral plate mesoderm to form the somitic bud (Christ et al., 1983). Furthermore, some somite cells migrate across the lateral somitic frontier and mix with LP cells (Nowicki et al., 2003). These somite cells constitute the abaxial region. We have previously reported that the rib in birds is composed of three compartments according to developmental dependencies on adjacent tissues (Aoyama et al., 2005). The proximal and vertebro-distal ribs correspond to the primaxial region, whereas the sterno-distal rib corresponds to the abaxial region (Burke and Nowicki, 2003). In the present study, although we could not distinguish primaxial and abaxial cells in vitro, both categories of cells have such common nature that they penetrate the lateral plate mesoderm at the thoracic level but not at the lumbar level. Consequently, in either case, our findings are consistent with the thoracic somite behavior in vivo.

3.4. Behavior of dermomyotome cells affected by cell-cell interaction in vitro

We expected that DM-th cells would continuously migrate forward after contact with LP-th cells and migrate backward after contact with LP-lu cells, similar to that observed for SC-th cells. However, in our in vitro system, the migratory behavior of DM cells that include the muscle anlagen was different from that of SC-th cells that include the rib anlagen. After contact with either LP-th or LP-lu cells, DM cells reversed the direction of migration (Fig. 10C, 5th, 7th, and 9th columns).

In vivo, DM-th cells migrate adhering to each other to form intercostal muscles, whereas DM-lu cells migrate individually to form the limb muscles (Chevallier, 1979; Jacob et al., 1979). In the present in vitro study, the cells were individually analyzed. This condition is different from that in vivo, where DM-th cells form a compact mass when they penetrate into the somatopleura. Rovasio et al. (1983) showed that neural crest cells exhibited oriented migration when they were cultured at high density, whereas they migrated randomly at a low density. DM-th cell mass could invade the LP, even though the LP cells repel single dermomyotome cell.

3.5. Behavior of lateral plate cells affected by cell-cell interaction in vitro

After contact with DM, which contains muscle primordia, LP-lu cells reversed their direction of migration (Fig. 10C, 8th and 10th columns). This migratory behavior of LP-lu may indicate the acceptance of invading muscle primordium. The 26th–28th somites, which are at lower thoracic or transition region (between thoracic and lumbar levels), become abdominal wall muscle (Yamaguchi, 2004), thus suggesting that the thoracic wall muscle primordium cells might penetrate into the abdominal wall.

After contact with SC-th cells that contain rib primordium, LP-lu cells did not change the direction of migration (Fig. 10C, 4th column). This migratory behavior of LP-lu may represent blocking the invasion of rib primordium. After contact with SC-th cells, LP-th cells changed their direction of migration (Fig. 10C, 2nd column).

This suggests that LP-th might allow the rib primordium to invade. These results are consistent with our unpublished data that the SC-th cells transplanted to the lumbar region do not invade the LP in vivo (Matsumori et al., unpublished).

3.6. Conclusion

This study showed that the behaviors of rib-forming SC-th cells were significantly different depending on whether the cells made contact with LP-th or LP-lu cells. SC-th cells migrated backward after contact with LP-lu cells. This phenomenon was considered to be caused by contact of thoracic somite cells with LP-lu cells. In normal development, chicken ribs grow laterally/ventrally, and then the sterno-distal ribs form pointing cranially but never enter the caudal–lumbar region. This may be explained by the repulsive intercellular interaction, which prevents SC-th cells from entering the lumbar somatic lateral plate. Thus, the cell–cell interaction presented here would assure that the rib forms only in the thoracic region.

4. Experimental procedures

4.1. Preparation of embryos

Fertilized eggs of White Leghorn chick were purchased from a local farm and incubated at 38 °C in a humidified incubator.

4.2. Isolation of explants from embryos

In the present study, “thoracic” indicated the 22nd–25th somite level, where the somites are origin of the 3rd–6th ribs, which possesses both vertebral and sternal ribs. DM-th and LP-th at the 21st somite-level was also used in some experiment. “Lumbar” indicated the 29th–31st somite level, where somites form the 3rd–6th lumbosacral vertebrae. A part of the embryo with the desired embryonic tissues was dissected and treated with 500 IU/mL dispase (Godo Shusei, Japan) in culture medium at 37 °C for 15–30 min, followed by isolation of each tissue using sharpened tungsten needles in Tyrode's saline. For culturing the cells, we used a 1:1 mix of Dulbecco's modified Eagle's medium (DMEM; Sigma-Aldrich) and Ham's F-10 (F10; Sigma-Aldrich), supplemented with 10% fetal calf serum (FCS) and 100 μg/mL kanamycin sulfate. A piece of SC was separated from DM. Although DM was separated carefully from SC, some SC cells may remain in the excised DM. Because SC is a mesenchymal tissue, it was difficult to remove it without destruction. Lateral half of DM was obtained by sagittally cutting DM in the middle. To isolate the somatic LP, it was cut at the border of somatic and splanchnic LP. SC-th and thoracic somatic lateral plate (LP-th) were dissected from HH-stage 17–18 (29–37 somite stage) chick embryos. DM-th, DM-lu and LP-lu were dissected from HH-stage 17–20 (29–41 somite stage) chick embryos.

4.3. RT-PCR

Total RNA was extracted using the RNeasy Mini Kit (QIAGEN). SC, DM, and LP at 21st–23rd somite level were obtained as mentioned above in Section 4.2. To examine the properties of explants, tissues from 7 embryos were processed immediately after excision. To examine the cells after culture, each tissue excised from 71 embryos was cultured for one day, cryopreserved, and processed.

Equal quantity of total RNA was subjected to semiquantitative RT using ReverTra Ace reverse transcriptase (TOYOBO, Japan). PCR was performed for 17–23 cycles of denaturation at 94 °C for 15 s, annealing at 60 °C for 30 s, and extension at 72 °C for 30 min using Ex-Taq polymerase (TaKaRa, Japan). The number of cycles for each primer set was determined within the linear range of amplification of target cDNA.

Primers used for PCR were as follows: Gapdh, 5′-AAAGTCGGAGT CAACGGATTTGG-3′ and 5′-GTTTCCCGTTCTCAGCCTTGA-3′; *Foxc2*, 5′-TGCCCTATTTAAGCGAGCAG-3′ and 5′-GTTCTGGATGGCCATAGTG ATG-3′; *Pax3*, 5′-GGTTTGGTTTAGCAACCGCC-3′, and 5′-ATCAGACAC GGCTTGCGG-3′; *Prx1*, 5′-CACTACCCCGATGCCTTTGT-3′ and 5′-AGGT ACTATGGGCTGCTCCA-3′. The amplified DNA fragments were electrophoresed on 5% acrylamide gels at 200 V for 30 min. DNA fragments were stained with a fluorescent dye, MIDORIGreen Advance (NIPPON genetics, Japan), and visualized under a blue light transilluminator.

4.4. Fluorescence staining

To trace cells in vitro, each explant was labeled with DiI or DiO (Invitrogen). The stock dye solutions (0.05%) were added to the culture medium at a final concentration of 0.01%. The culture medium consisted of DMEM:F10 = 1:1 supplemented with 10% FCS and 100 μg/mL kanamycin sulfate. The isolated tissues were incubated in the dye solution at 37 °C in 5% CO_2/air for 20 min, followed by rinsing five times with Tyrode's saline to remove unconjugated dye.

4.5. Co-culture experiment on a 2D substrate

Explants of somites and its derivatives were co-cultured with explants of LP in a glass-base dish (3911-035 Iwaki, Japan) with the culture medium at 37 °C under 5% CO_2/air. A pair of explants was placed with a spacing of 1 mm between the explants. The explants settled and proliferated on the substrate. Cells migrated away from the explants and made contact with each other halfway between the explants.

4.6. Co-culture experiment on a 1D substrate

The explants were co-cultured in a semisolid medium on CytoGraph (DNP, Japan) type L10S300 with 10-μm wide hydrophilic paths intervening with 300-μm wide hydrophobic areas. The semisolid medium was composed of DMEM:F10 = 1:1, 15% FCS, 100 μg/mL kanamycin sulfate, and 1.7% methylcellulose 4000 (Chameleon Reagent). The hydrophobic areas were constructed by coating with tetraethylene glycol layer, and hydrophilic paths were uncovered glass surface (Okochi et al., 2009). The substrate was treated with 3% bovine serum albumin (Sigma-Aldrich) for blocking excess cell adhesion before culture.

4.7. Time-lapse imaging

The cultured cells were observed under a phase-contrast microscope (IX71, Olympus, Japan) with a 4× or 10× objective and photographed every 1 min for 48 h with a camera (Eos Kiss X6i, Canon, Japan) controlled by EOS Utility (Canon, Japan).

4.8. Cell tracking

We analyzed cell migration using consecutive photographs captured every 10 min for 60 min before and after contact between the co-culture cells. The cultured cells migrated away from the explants; co-cultured cells approached each other, and finally made contact. In this study, we named the preceding tip of the migrating cell as the leading edge and the rear tip as the trailing edge. These names were defined according to the initial direction of cell migration and we did not rename when the cells changed their direction of migration. On consecutive photographs, we manually marked the leading and trailing edges (Fig. 3D), and their positions were recorded in X–Y coordinates of pixels using ImageJ Multi-point Analyze Tool (NIH, USA). Then, we calculated the migration velocity (μm/min) from the distance between the marked points using Numbers (Apple) and Excel (Microsoft).

4.9. Statistical analysis

Statistical analysis was performed using R (R Development Core Team, Vienna, Austria). The migration velocity was compared by Student's *t*-test ($P > 0.05$, by F test) or the Wilcoxon rank sum test ($P \leq 0.05$, by F test). Comparison of the ratio of cell length after to before contact was performed by paired *t*-test. To compare the ratios of cell length after contact, we used Student's *t*-test ($P > 0.05$, by F test) or the Wilcoxon rank sum test ($P \leq 0.05$, by F test). We divided each 60-min period before and after contact into two periods of 30 min each. Velocity distribution patterns in each period were grouped by hierarchical clustering analysis using the Ward's method. The Ward's method is an agglomerative method based on a sum of squares criterion (Murtagh and Legendre, 2014). Observations in each cluster were agglomerated to minimize the extra sum of squares at each clustering step. Distance obtained by criterion of the Ward's method represented the height of dendrograms.

Acknowledgement

Part of this study was supported by JSPS KAKENHI Grant Numbers JP23590219, JP26460254.

References

Abercrombie, M., 1970. Contact inhibition in tissue culture. In Vitro 6, 128–142. https://doi.org/10.1007/BF02616114.
Abercrombie, M., Heaysman, J.E.M., 1954. Observations on the social behaviour of cells in tissue culture. II. Monolayering of fibroblasts. Exp. Cell Res. 6, 293–306. https://doi.org/10.1016/0014-4827(54)90176-7.
Aoyama, H., 1993. Developmental plasticity of the prospective dermatome and the prospective sclerotome region of an avian somite. Develop. Growth Differ. 35, 507–519. https://doi.org/10.1111/j.1440-169X.1993.00507.x.
Aoyama, H., Asamoto, K., 1988. Determination of somite cells: independence of cell-differentiation and morphogenesis. Development 104, 15–28.
Aoyama, H., Asamoto, K., 2000. The developmental fate of the rostral/caudal half of a somite for vertebra and rib formation: experimental confirmation of the re-segmentation theory using chick-quail chimeras. Mech. Dev. 99, 71–82. https://doi.org/10.1016/S0925-4773(00)00481-0.
Aoyama, H., Mizutani-Koseki, Y., Koseki, H., 2005. Three developmental compartments involved in rib formation. Int. J. Dev. Biol. 49, 325–333. https://doi.org/10.1387/ijdb.041932ha.
Bellairs, R., Sanders, E.J., Portch, P.A., 1980. Behavioural properties of chick somitic mesoderm and lateral plate when explanted *in vitro*. J. Embryol. Exp. Morphol. 56, 41–58.
Buffinger, N., Stockdale, F.E., 1994. Myogenic specification in somites: induction by axial structures. Development 120 (6), 1443–1452.
Burke, A.C., Nowicki, J.L., 2003. A new view of patterning domains in the vertebrate mesoderm. Dev. Cell 4, 159–165. https://doi.org/10.1016/S1534-5807(03)00033-9.
Carmona-Fontaine, C., Matthews, H.K., Kuriyama, S., Moreno, M., Dunn, G.A., Parsons, M., Stern, C.D., Mayor, R., 2008. Contact inhibition of locomotion *in vivo* controls neural crest directional migration. Nature 456, 957–961. https://doi.org/10.1038/nature07441.
Carter, S.B., 1965. Principles of cell motility: the direction of cell movement and cancer invasion. Nature 208, 1183–1187. https://doi.org/10.1038/2081183a0.
Chevallier, A., 1979. Role of the somitic mesoderm in the development of the thorax in bird embryos. II. Origin of thoracic and appendicular musculature. J. Embryol. Exp. Morphol. 49, 73–88.
Christ, B., Ordahl, C.P., 1995. Early stages of chick somite development. Anat. Embryol. 191, 381–396. https://doi.org/10.1007/BF00304424.
Christ, B., Jacob, M., Jacob, H.J., 1983. On the origin and development of the ventrolateral abdominal muscles in the avian embryo. An experimental and ultrastructural study. Anat. Embryol. 166, 87–101. https://doi.org/10.1007/BF00317946.
Christ, B., Brand-Saberi, B., Grim, M., Wilting, J., 1992. Local signaling in dermomyotomal cell type specification. Anat. Embryol. 186, 505–510.
Cousin, H., 2017. Cadherins function during the collective cell migration of Xenopus cranial neural crest cells: revisiting the role of E-cadherin. Mech. Dev. 148, 79–88. https://doi.org/10.1016/j.mod.2017.04.006.
Davis, J.R., Huang, C.Y., Zanet, J., Harrison, S., Rosten, E., Cox, S., Soong, D.Y., Dunn, G.A., Stramer, B.M., 2012. Emergence of embryonic pattern through contact inhibition of locomotion. Development 139, 4555–4560. https://doi.org/10.1242/dev.082248.
Davis, J.R., Luchici, A., Mosis, F., Thackery, J., Salazar, J.A., Mao, Y., Dunn, G.A., Betz, T., Miodownik, M., Stramer, B.M., 2015. Inter-cellular forces orchestrate contact inhibition of locomotion. Cell 161, 361–373. https://doi.org/10.1016/j.cell.2015.02.015.
Dockter, J., Ordahl, C.P., 2000. Dorsoventral axis determination in the somite: a re-examination. Development 127, 2201–2206.
Ellison, M.L., Ambrose, E.J., Easty, G.C., 1969a. Chondrogenesis in chick embryo somites *in vitro*. J. Embryol. Exp. Morphol. 21, 331–340.
Ellison, M.L., Ambrose, E.J., Easty, G.C., 1969b. Myogenesis in chick embryo somites *in vitro*. J. Embryol. Exp. Morphol. 21, 341–346.
Erickson, C.A., 1985. Control of neural crest cell dispersion in the trunk of the avian embryo. Dev. Biol. 111, 138–157. https://doi.org/10.1016/0012-1606(85)90442-7.
Funayama, N., Sato, Y., Matsumoto, K., Ogura, T., Takahashi, Y., 1999. Coelom formation: binary decision of the lateral plate mesoderm is controlled by the ectoderm. Development 126, 4129–4138.
Hamburger, V., Hamilton, H.L., 1951. A series of normal stages in the development of the chick embryo. J. Morphol. 88, 49–92. https://doi.org/10.1002/jmor.1050880104.
Hernandez-Fleming, M., Rohrbach, E.W., Bashaw, G.J., 2017. Sema-1a reverse signaling promotes midline crossing in response to secreted semaphorins. Cell Rep. 18, 174–184. https://doi.org/10.1016/j.celrep.2016.12.027.
Huang, R.J., Zhi, Q.X., Schmidt, C., Wilting, J., Brand-Saberi, B., Christ, B., 2000. Sclerotomal origin of the ribs. Development 127, 527–532.
Jacob, M., Christ, B., Jacob, H.J., 1979. The migration of myogenic cells from the somites into the leg region of avian embryos. Anat. Embryol. (Berl) 157, 291–309.
Jotereau, F.V., Le Douarin, N.M., 1982. Demonstration of a cyclic renewal of the lymphocyte precursor cells in the quail thymus during embryonic and perinatal life. J. Immunol. 129, 1869–1877.
Kato, N., Aoyama, H., 1998. Dermomyotomal origin of the ribs as revealed by extirpation and transplantation experiments in chick and quail embryos. Development 125, 3437–3443.
Kenny-Mobbs, T., Thorogood, P., 1987. Autonomy of differentiation in avian brachial somites and the influence of adjacent tissues. Development 100, 449–462.
Kieny, M., Sengel, P., Mauger, A., 1972. Early regionalization of somitic mesoderm as studied by development of axial skeleton of chick embryo. Dev. Biol. 28, 142–161. https://doi.org/10.1016/0012-1606(72)90133-9.
Kridsada, K., Niu, J.W., Haldipur, P., Wang, Z.P., Ding, L., Li, J.J., Lindgren, A.G., Herrera, E., Thomas, G.M., Chizhikov, V.V., Millen, K.J., Luo, W.Q., 2018. Roof plate-derived radial glial-like cells support developmental growth of rapidly adapting mechanoreceptor ascending axons. Cell Rep. 23, 2928–2941. https://doi.org/10.1016/j.celrep.2018.05.025.
Kuratani, S., Martin, J.F., Wawersik, S., Lilly, B., Eichele, G., Olson, E.N., 1993. The expression pattern of the chick homeobox gene gMHox suggests a role in patterning of the limbs and face and in compartmentalization of somites. Dev. Biol. 161, 357–369. https://doi.org/10.1006/dbio.1994.1037.
Laumonnerie, C., Tong, Y.G., Alstermark, H., Wilson, S.I., 2015. Commissural axonal corridors instruct neuronal migration in the mouse spinal cord. Nat. Commun. 6 (7028), 1–14. https://doi.org/10.1038/ncomms8028.
Le Douarin, N.M., 1984. Cell migrations in embryos. Cell 38, 353–360.
Liem, I.K., Aoyama, H., 2009. Body wall morphogenesis: limb-genesis interferes with body wall-genesis via its influence on the abaxial somite derivatives. Mech. Dev. 126, 198–211. https://doi.org/10.1016/j.mod.2008.11.003.
de la Loza, M.C.D., Diaz-Torres, A., Zurita, F., Rosales-Nieves, A.E., Moeendarbary, E., Franze, K., Martin-Bermudo, M.D., González-Reyes, A., 2017. Laminin levels regulate tissue migration and anterior-posterior polarity during egg morphogenesis in Drosophila. Cell Rep. 20, 211–223. https://doi.org/10.1016/j.celrep.2017.06.031.
Mayor, R., Etienne-Manneville, S., 2016. The front and rear of collective cell migration. Nat. Rev. Mol. Cell Bio. 17, 97–109. https://doi.org/10.1038/nrm.2015.14.
Monsoro-Burq, A.H., 2005. Sclerotome development and morphogenesis: when experimental embryology meets genetics. Int. J. Dev. Biol. 49, 301–308. https://doi.org/10.1387/ijdb.041953am.
Murtagh, F., Legendre, P., 2014. Ward's hierarchical agglomerative clustering method: which algorithms implement Ward's criterion? J. Classif. 31, 274–295. https://doi.org/10.1007/s00357-014-9161-z.
Nowicki, J.L., Burke, A.C., 2000. Hox genes and morphological identity: axial versus lateral patterning in the vertebrate mesoderm. Development 127, 4265–4275.
Nowicki, J.L., Takimoto, R., Burke, A.C., 2003. The lateral somitic frontier: dorso-ventral aspects of anterio-posterior regionalization in avian embryos. Mech. Dev. 120, 227–240. https://doi.org/10.1016/S0925-4773(02)00415-X.
Okochi, N., Okazaki, T., Hattori, H., 2009. Encouraging effect of cadherin-mediated cell-cell junctions on transfer printing of micropatterned vascular endothelial cells. Langmuir 25, 6947–6953. https://doi.org/10.1021/la9006668.
Ordahl, C.P., Le Douarin, N.M., 1992. Two myogenic lineages within the developing somite. Development 114, 339–353.
Pourquié, O., Coltey, M., Teillet, M.A., Ordahl, C., Le Douarin, N.M., 1993. Control of dorsoventral patterning of somitic derivatives by notochord and floor plate. PNAS. 90, 5242–5246. https://doi.org/10.1073/pnas.90.11.5242.
Reig, G., Pulgar, E., Concha, M.L., 2014. Cell migration: from tissue culture to embryos. Development 141, 1999–2013. https://doi.org/10.1242/dev.101451.
Rovasio, R.A., Delouvee, A., Yamada, K.M., Timpl, R., Thiery, J.P., 1983. Neural crest cell migration: requirements for exogenous fibronectin and high cell density. J. Cell Biol. 96, 462–473. https://doi.org/10.1083/jcb.96.2.462.
Scarpa, E., Mayor, R., 2016. Collective cell migration in development. J. Cell Biol. 212, 143–155. https://doi.org/10.1083/jcb.201508047.
Scarpa, E., Roycroft, A., Theveneau, E., Terriac, E., Piel, M., Mayor, R., 2013. A novel method to study contact inhibition of locomotion using micropatterned substrates. Biol. Open 2, 901–906. https://doi.org/10.1242/bio.20135504.
Scarpa, E., Szabo, A., Bibonne, A., Theveneau, E., Parsons, M., Mayor, R., 2015. Cadherin switch during EMT in neural crest cells leads to contact inhibition of locomotion via repolarization of forces. Dev. Cell 34, 421–434. https://doi.org/10.1016/j.devcel.2015.06.012.
Scarpa, E., Roycroft, A., Theveneau, E., Terriac, E., Piel, M., Mayor, R., 2016. A novel method to study contact inhibition of locomotion using micropatterned substrates (vol 2, pg 901). Biol. Open 5, 1553. https://doi.org/10.1242/bio.020917.
Shearman, R.M., Burke, A.C., 2009. The lateral somitic frontier in ontogeny and phylogeny. J. Exp. Zool. Part B. 312B, 603–612. https://doi.org/10.1002/jez.b.21246.
Stern, H.M., Hauschka, S.D., 1995. Neural tube and notochord promote *in vitro* myogenesis in single somite explants. Dev. Biol. 167, 87–103. https://doi.org/10.1006/dbio.1995.1009.
Stramer, B., Moreira, S., Millard, T., Evans, I., Huang, C.Y., Sabet, O., Milner, M., Dunn, G., Martin, P., Wood, W., 2010. Clasp-mediated microtubule bundling regulates persistent motility and contact repulsion in Drosophila macrophages *in vivo*. J. Cell Biol. 189, 681–689. https://doi.org/10.1083/jcb.200912134.
Sudo, H., Takahashi, Y., Tonegawa, A., Arase, Y., Aoyama, H., Mizutani-Koseki, Y., Moriya, H., Wilting, J., Christ, B., Koseki, H., 2001. Inductive signals from the somatopleure mediated by bone morphogenetic proteins are essential for the formation of the sternal component of avian ribs. Dev. Biol. 232, 284–300. https://doi.org/10.1006/dbio.2001.0198.
Takeichi, M., 2014. Dynamic contacts: rearranging adherens junctions to drive epithelial remodelling. Nat. Rev. Mol. Cell Bio. 15, 397–410. https://doi.org/10.1038/nrm3802.
Theveneau, E., Marchant, L., Kuriyama, S., Gull, M., Moepps, B., Parsons, M., Mayor, R., 2010. Collective chemotaxis requires contact-dependent cell polarity. Dev. Cell 19, 39–53. https://doi.org/10.1016/j.devcel.2010.06.012.
Villar-Cerviño, V., Molano-Mazón, M., Catchpole, T., Valdeolmillos, M., Henkemeyer, M., Martinez, L.M., Borrell, V., Marin, O., 2013. Contact repulsion controls the dispersion

and final distribution of Cajal-Retzius cells. Neuron 77, 457–471. https://doi.org/10.1016/j.neuron.2012.11.023.
Wang, H.U., Anderson, D.J., 1997. Eph family transmembrane ligands can mediate repulsive guidance of trunk neural crest migration and motor axon outgrowth. Neuron 18, 383–396. https://doi.org/10.1016/S0896-6273(00)81240-4.
Williams, B.A., Ordahl, C.P., 1997. Emergence of determined myotome precursor cells in the somite. Development 124, 4983–4997.
Yamaguchi, M., 2004. Origin of body wall muscles in birds (in Japanese), Thesis of Master of Science. Osaka University.